Quiet-time statistics: A tool to probe the dynamics of self-organized-criticality systems from within the strong overlapping regime

R. Sánchez
Departamento de Física, Universidad Carlos III de Madrid, 28911 Leganés, Madrid, Spain

D. E. Newman and W. Ferenbaugh
Department of Physics, University of Alaska—Fairbanks, Fairbanks, Alaska 99709

B. A. Carreras and V. E. Lynch
Fusion Energy Division, Oak Ridge National Laboratory, Oak Ridge, Tennessee 37831-8070

B. Ph. van Milligen
Laboratorio Nacional de Fusión, Asociación Euratom-CIEMAT, 28040 Madrid, Spain
(Received 10 May 2002; published 23 September 2002)

A method is presented that allows one to obtain information about the underlying dynamics of a self-organized-criticality system even when the strong-overlapping or hydrodynamic regime (in which individual avalanches are no longer distinguishable) is the only one amenable of probing. The method is based on the analysis of the statistics of the lapses of time between activity bursts or quiet times. The case of a randomly driven running sandpile is used to illustrate the use and capabilities of this technique.

DOI: 10.1103/PhysRevE.66.036124 PACS number(s): 05.65.+b, 45.70.−n, 52.25.Fi

I. INTRODUCTION

Self-organized criticality (SOC) [1] is a concept that has found wide application in the physical and earth sciences in the last 15 years [2–10]. Due to limits in the available computing power, much of the theoretical work on this concept has been done with cellular automata models, of which the sandpile is probably the best known example [11–14,15–18]. In it, sand is dropped following some prescribed rule. Then, whenever the slope (or the height) at some cell exceeds a prescribed threshold value, it becomes unstable and relaxes by moving part of its content to the neighboring cell or cells. These can themselves go unstable, and the relaxation can propagate forming an avalanche. The rules that govern both the driving and the relaxation processes distinguish the different sandpile models. But in all of them, a steady state is reached after the flux of sand that leaves through the bottom of the sandpile balances the incoming drive. This final state shares many of the characteristics of critical points from equilibrium phase transition theory. Namely, self-similarity and correlations that diverge with the system size [19].

Self-similarity can be easily made apparent in SOC systems by constructing the probability distribution function (PDF) of, say, the sizes of the avalanches. These PDFs exhibit power laws that extend for several decades and decay with an exponent slower than -2, which makes the distribution not have a finite variance (it diverges instead with the system size) [19]. However, it is necessary to be able to distinguish single avalanches in order to perform this type of analysis. This is ensured in most sandpile models studied in the literature by halting the drive after an avalanche is excited. It is again restarted only after all avalanche activity has disappeared throughout the system.

Regretfully, in a real system, the drive does not wait for any activity to cease. There is always a finite (even if sometimes negligible) probability of avalanche overlapping, which will increase with the strength of the drive. Therefore, any analysis based on the construction of any of these PDFs may be difficult to interpret, and sometimes even turn useless, after the system has entered the hydrodynamic regime [13]. This is a situation of more than just academic interest. For instance, in the case of the occurrence of turbulent transport in a plasma magnetically confined in a tokamak or a stellarator (systems for which a SOC paradigm has been recently proposed, which accounts for some of the phenomenology experimentally observed [9,10]), it might very well be that the hydrodynamic regime is the only one relevant to the experiment [20,21]. Therefore, developing analysis tools to investigate the underlying system dynamics in the presence of strong overlapping is of interest.

In this paper, we consider the possible use of quiet-time statistics to perform this task. Quiet-time statistics are somewhat related to waiting-time statistics, which have been recently revisited in the context of SOC dynamics by several authors [14,22,23]. But quiet times can be shown not to suffer from the same shortcomings as their relatives [24]. To explore the possibilities of this tool, we have applied it to the analysis of the running sandpile [11,13], which is the simplest SOC system exhibiting avalanche overlapping. The paper is organized as follows. In Sec. II, some properties regarding the waiting times of a uniform Poisson point process are introduced, which will be relevant to the rest of our discussion. The application of these ideas to the running sandpile will take us to the definition of the quiet-time concept in Sec. III. In Sec. IV, quiet-time statistics will be applied to probe the underlying dynamics of the running sandpile from within the strong overlapping regime. The usefulness of this technique to capture the underlying SOC dynamics will be tested against results obtained from an equivalent sandpile

where no avalanche overlapping is allowed. Finally, some conclusions will be drawn in Sec. VI.

II. WAITING TIMES OF A POISSON POINT PROCESS

A point process is an ordered set of events, with zero duration, that are consecutively triggered in time [25]. It can be represented by a semi-infinite series of real numbers P formed by those instants of time at which events are triggered:

$$P \equiv \{t_k \in [0,\infty), \quad k=1,2,3,\ldots\}, \tag{1}$$

where the initial time at which data recording begins has been set arbitrarily to $t=0$.

Associated to process P, a second semi-infinite series is defined in the following way:

$$W^P \equiv \{w_k = t_{k+1} - t_k, k=1,2,3,\ldots\}. \tag{2}$$

W^P will be referred to as the *waiting-time* series associated to P. A point process is called a uniform Poisson process if the probability of any waiting time in its associated W^P series exceeding some prescribed value satisfies [26]

$$\frac{p(w>t+s)}{p(w>s)} = p(w>t), \quad \forall \ t,s>0. \tag{3}$$

It is important to notice that Eq. (3) implies the absence of any temporal correlation between triggerings. In more physical terms, it can be restated by saying that the system where P takes place behaves in the same way no matter which reference time is chosen to look at it, as should be expected from the lack of memory of the dynamics. Since Eq. (3) can be rewritten as

$$p(w>t+s) = p(w>s)p(w>t), \tag{4}$$

this probability can be expressed in the form

$$p(w>s) = e^{-\sigma s} \tag{5}$$

for some $\sigma>0$. From Eq. (5), it follows that the PDF of the waiting times (from now on, all PDFs will be represented with P, in contrast to probabilities with p) is given by

$$P^P_{wait}(w) = \sigma e^{-\sigma w}. \tag{6}$$

This PDF characterizes completely the Poisson process [26]. σ is known as the mean rate of the process and $1/\sigma$ gives the average waiting time between triggerings.

Several theorems regarding Poisson processes that will be used later are now presented. The first two are well-known results from the theory of Poisson processes, and are thus stated without proof (see, for instance, Ref. [26] for a mathematical proof).

Theorem 1. *Any* new process P_p formed by *randomly* choosing elements in P with some probability p is again a Poisson process, with mean rate given by $\sigma_p = \sigma p$.

Theorem 2. *Any* new series formed by *randomly* choosing elements in W^P with any probability follows the same PDF as the whole series given by Eq. (6). This theorem is particularly useful when trying to estimate σ in practice.

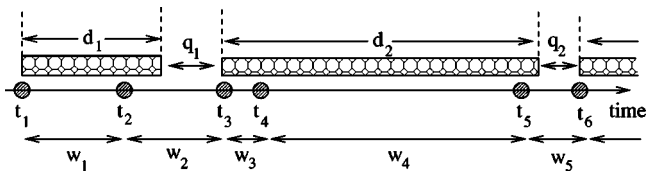

FIG. 1. Sketch explaining the different series associated with the Poisson process P: the waiting time series W^P and the quiet-time series Q^P_D.

The third one is a result, which refers to another series Q^P_D, that can be constructed from a Poisson process P. The procedure goes as follows: at time $t_1 \in P$ some real number $d_1>0$ is chosen. Then, the first element in Q^P_D is given by (see Fig. 1)

$$q_1 = t_{s_{(1)}} - (t_1 + d_1) = \sum_{l=1}^{s_{(1)}-1} w_l - d_1, \tag{7}$$

$s_{(1)}$ being the *lowest* positive integer verifying that $t_{s_{(1)}} > t_1 + d_1$. The next element in Q^P_D is computed in an identical way: a second real number d_2 is chosen at time $t_{s_{(1)}}$, and the second element in Q^P_D is obtained as

$$q_2 = t_{s_{(2)}} - (t_{s_{(1)}} + d_2) = \sum_{l=s_{(1)}}^{s_{(2)}-1} w_l - d_2, \tag{8}$$

where $s_{(2)}$ is again defined as the lowest positive integer which verifies that $t_{s_{(2)}} > t_{s_{(1)}} + d_2$. This process is continued till arbitrarily large k,

$$q_k = t_{s_{(k)}} - (t_{s_{(k-1)}} + d_k) = \sum_{l=s_{(k-1)}}^{s_{(k)}-1} w_l - d_k, \tag{9}$$

with $s_{(k)}$ being the lowest positive integer for which $t_{s_{(k)}} > t_{s_{(k-1)}} + d_k$. Denoting the set formed by all d_k by D, and the PDF according to which elements in D are distributed by $P_D(d)$, the third theorem can be stated as follows.

Theorem 3. The elements in Q^P_D are also distributed according to P^P_{wait}.

Proof. To prove it, it is sufficient to realize that any possible q must be equal to the sum of a real number d [from the distribution $P_D(d)$] and some finite number N of consecutive waiting times [each of them distributed according to $P^P_{wait}(w)$]. For any particular series of waiting times and fixed q and d, N is equal to the order number of the last waiting time satisfying

$$w_N = q + d - \sum_{k=1}^{N-1} w_k > 0. \tag{10}$$

Let us assume now that, for fixed d and N, the probability of any possible collection of waiting-time values can be described by some function $p_d(w_1, w_2, w_3, \ldots, w_{N-1})$, which contains any possible correlation between d and the $\{w_i\}$

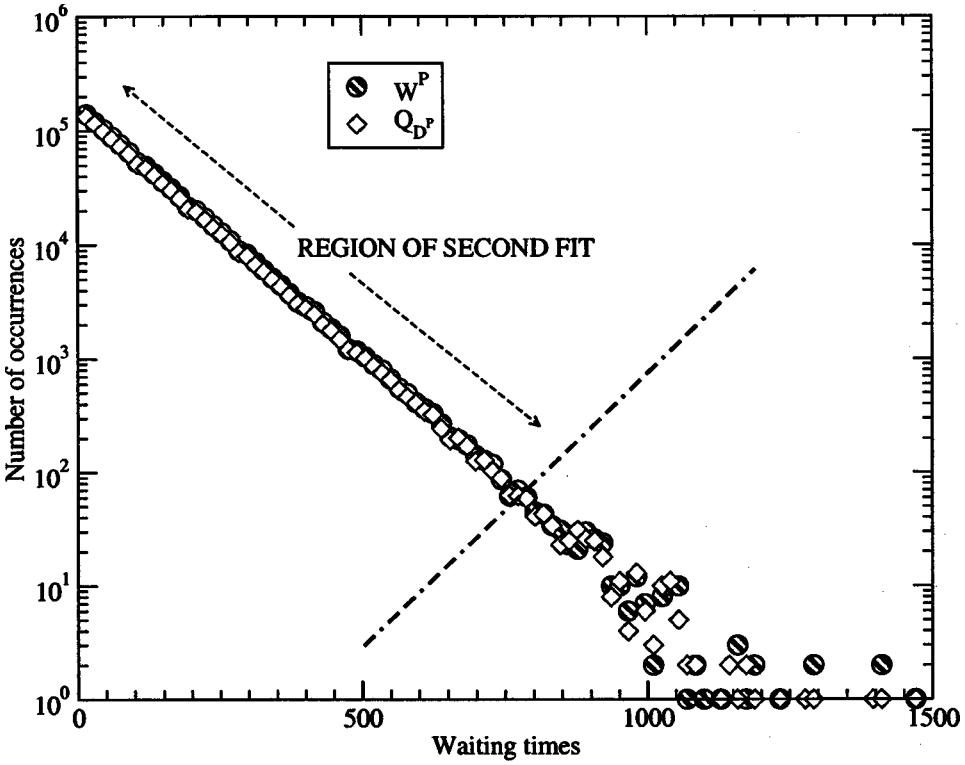

FIG. 2. Comparison of the PDFs according to which the elements in W^P and Q_D^P are distributed for the Poisson process P described in Sec. II of the text. Both waiting times and quiet times are measured in iterations in this and all other figures.

collection (it would be constant in the case of no correlation). Then, the probability of appearance of some value of q for fixed d and N is given by

$$p_d^{[N]}(q)=\sigma^N e^{-\sigma(q+d)}K_N(d), \tag{11}$$

where the kernel $K_N(d)$ is defined by

$$K_N(d)\equiv\int_0^d dw_1\int_0^{d-w_1} dw_2\cdots\int_0^{d-\sum_{l=1}^{N-2}w_l} dw_{N-1}\; p_d \times(w_1,w_2,w_3,\ldots,w_{N-1}). \tag{12}$$

The total probability of obtaining q is now computed by, first, summing $p_d^{[N]}(q)$ over all possible N and averaging it over all possible d values,

$$\int_0^\infty dd' P_D(d')\sum_{N=1}^\infty p_{d'}^{[N]}(q) = e^{-\sigma q}\left(\int_0^\infty dd' P_D(d')\sum_{N=1}^\infty \sigma^N e^{-\sigma d'}K_N(d')\right), \tag{13}$$

and, second, normalizing it to unity over all possible q's. This normalization eliminates the constant bracketed factor from the right-hand side of Eq. (13), except for a σ factor. The PDF according to which the elements in Q_D^P are distributed is finally given by

$$P_Q^{[P,D]}(q)=\sigma\; e^{-\sigma q}=P_{wait}^P(q), \tag{14}$$

as the theorem states.

It is easy to test Eq. (14) numerically. To do it, a Poisson point process P has been obtained by generating a series of random numbers in $[0,1]$, and storing the order number of those that exceed a given threshold, $0<t<1$. P clearly satisfies the independence condition required for Eq. (5) to hold and, as expected, its associated W^P series is distributed according to an exponential PDF. Using $t=0.99$ (see Fig. 2) and fitting to an exponential law, a mean rate $\sigma=0.009\,56 \pm 0.000\,16$ is obtained. This value is within 5% of the theoretical $\sigma=1-t=0.1$. Other tests (with different values for t) suggest that the typical deviation that should be expected lies within 1–10 % from the theoretical value. The reason for this discrepancy is to be found in the worse statistics of the longest waiting times. When the previous fit is recalculated excluding them, a much closer value is obtained, $\sigma=0.010\,059\pm 0.000\,048$, less than 0.5% from the theoretical value.

If we repeat the exercise with the Q_D^T series [generated following Eq. (9)] using values for $d\in[0,100]$ produced by a random number generator, almost identical results are obtained. The associated PDF has been included in the same figure for easier comparison. Clearly, both PDFs are identical: the exponent obtained for the Q_D^T distribution is $\sigma=0.009\,475\pm 0.000\,18$, again around a 5% from the theoretical σ, and $\sigma=0.009\,991\,1\pm 0.000\,03$ (less than 0.1%) when the longest values are discarded.

III. QUIET TIMES IN A RUNNING SANDPILE

The running sandpile [11,13] is the simplest SOC system that exhibits avalanche overlapping. It is composed of L cells, each of them storing an amount of sand h_k, with k being any integer in $[1,L]$. Avalanches can be excited when-

ever the local slope $Z_k \equiv h_{k+1} - h_k$ exceeds a prescribed critical threshold Z_c at any cell. Then, N_f grains of sand are moved from the unstable cell to the next cell downhill. If the receiving cell becomes unstable itself, the avalanche can then propagate.

The sandpile is driven randomly by dropping one grain of sand with some prescribed probability p_0 at each iteration and on each cell. This is done by generating a random number in $[0,1]$ per cell and iteration. Whenever this number exceeds $1-p_0$, a grain of sand is dropped. Interestingly, this procedure is identical to that used to generate the test Poisson process in the preceding section. The mean rate is however $p_0 L$ in the present case, since at each iteration L different numbers are produced, one per cell.

It is essential to notice now that a grain of sand must be dropped at the same cell and iteration at which any avalanche is triggered. But not every drop that falls gives rise to an avalanche. If p_s denotes the probability for an avalanche to be triggered in one cell when a drop falls, Theorem 1 from the preceding section guarantees that the ordered series formed by the iterations at which avalanches are triggered,

$$T \equiv \{i_k \in Z^+, k = 1,2,3, \ldots\}, \tag{15}$$

must necessarily inherit the Poisson character of the drive, with mean rate $\sigma_0 = p_s p_0 L$. Therefore, if σ_0 could be somehow measured, it would provide us with an accurate estimation of the dependences and scalings of p_s with the system parameters, as well as many other interesting quantities characterizing the running sandpile dynamics.

In principle, σ_0 might be estimated from the W^T series associated with T, which must follow an exponential law with exponent σ_0. However, the running sandpile is more complex than a Poisson point process. All avalanches in the sandpile have a finite duration, $d>0$. Therefore, as soon as σ_0 increases, the probability also increases for any triggering in T to be excited before the previous avalanche has died away. For large enough σ_0, the system enters into the hydrodynamic regime where avalanche overlapping happens frequently, and the number of elements in T that cannot be detected increases. What can be measured in practice is a subset of T:

$$A^T \equiv \{a_l = t_{k_l} \in T, l = 1,2,3, \ldots\}, \tag{16}$$

with $\{k_1, k_2, \ldots, k_j, \ldots\}$ being the subset of indices of the iterations at which avalanche activity has started. (For instance, considering again the triggering process shown in Fig. 1, and d_1 and d_2 being the durations of the avalanches triggered at times t_1 and t_3, the triggerings taking place at times t_2, t_4, and t_5 would not be detectable. The A^T series for this process would begin with $a_1 = t_1$, $a_2 = t_3$, and $a_3 = t_6$.) Notice that $A^T \subseteq T$, but the identity is only reached in the limit $\sigma_0 \to 0$. A^T will be referred to as the "avalanching process" associated to the T process, from now on referred to as the "triggering process."

In general, it is very difficult to extract useful information about the underlying process T from the waiting-time series associated with A (in spite of this, slightly different flavors of this PDF have been often used in the literature [22–24]):

$$W^A \equiv \{w_k^A = a_{k+1} - a_k, k = 1,2,3, \ldots\}, \tag{17}$$

since they are not necessarily distributed according to an exponential law. But to prove this, we must first deal with the avalanche duration PDF. According to one of the hallmarks of SOC dynamics, these durations are distributed according to a power-law-like distribution in the limit of σ_0 (or p_0) $\to 0$. This distribution is well approximated by the following functional form [19]:

$$P_D(d, \sigma_0 \to 0) \simeq \frac{e^{-d/d_1}}{1 + (d/d_2)^k}, \tag{18}$$

$k>0$ being the power-law exponent. d_1 and d_2 are two functions of L, the system size which verifies that

$$\lim_{L \to \infty} d_1(L) = \infty, \quad \lim_{L \to \infty} d_2(L) = 0. \tag{19}$$

They model the limitations to self-similarity induced on the distribution by the finite size of the system. Roughly speaking, self-similarity is limited to those time scales lying between them. In the presence of overlapping, this PDF can however be deformed due to the nontrivial changes induced by the spatial interaction of avalanches in their well-established spatial structure [27]. In particular, the power-law exponent of the PDF can change or even disappear, and its self-similarity limits can be shifted, as shown, for instance, in Fig. 3. Therefore, this σ_0 dependence will be made explicit by denoting the avalanche duration PDF by $P_D(d, \sigma_0)$ in what follows.

It is now straightforward to show that the probability for any w^A (that when properly normalized to unity over $[0,\infty)$ gives the PDF) does not follow an exponential law but instead,

$$p(w^A) = \sigma_0 e^{-\sigma_0 w^A} H(w^A, \sigma_0), \tag{20}$$

with the function $H(w^A, \sigma_0)$ defined by

$$H(w^A, \sigma_0) \equiv \int_0^{w^A} ds P_D(s, \sigma_0) e^{\sigma_0 s}. \tag{21}$$

As might be expected, $H(w^A, \sigma_0) \to 1$ only when $\sigma_0 \to 0$, which makes this PDF of little use in order to estimate σ_0 as soon as the hydrodynamic regime is entered. As an illustration, Fig. 4 shows the PDF according to which values in W^A are distributed for a series of sandpile runs with increasing p_0 (and therefore, increasing σ_0). It is apparent how, for the smallest σ_0's, the PDF stays close to an exponential above a certain minimum value for w^A that vanishes with σ_0. However, as σ_0 increases, it quickly departs from the exponential law, which makes impossible the determination of σ_0.

However, Theorem 3 from the preceding section provides us with an easy and elegant alternative solution for this problem. It is sufficient to construct the Q_D^T process from T using

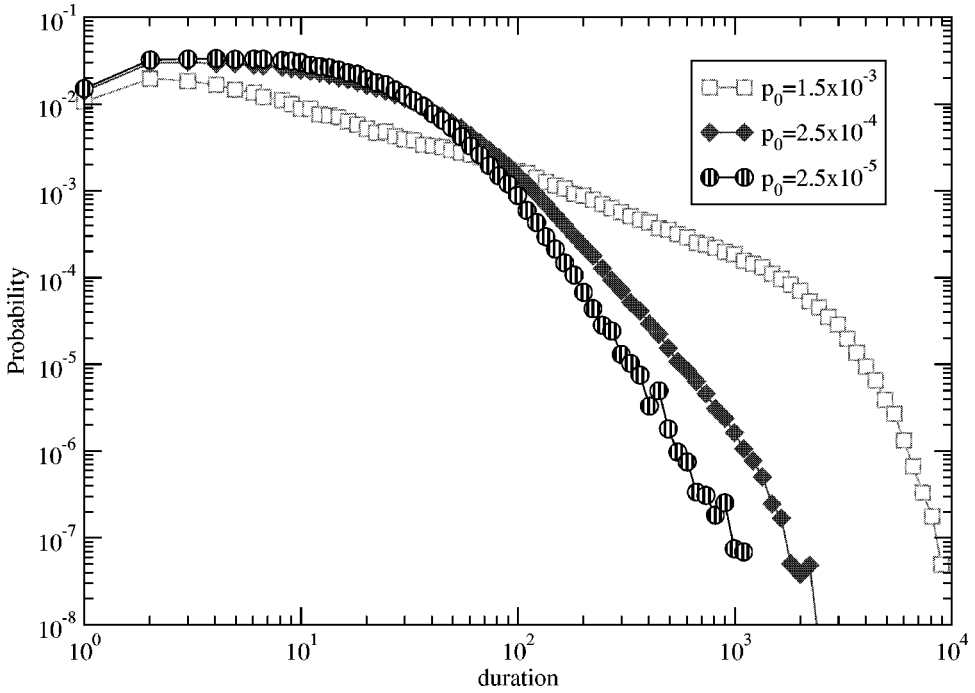

FIG. 3. Change of $P_D(d,\sigma_0)$ with drive strength (in this case with p_0, since $\sigma_0 = p_s p_0 L$) for a sandpile run with $L=400$, $Z_c=20$, and $N_f=3$. In this and all other figures, duration units are iterations, and both p_0 and σ_0 units are iterations^{-1}.

Eq. (9), with the set D being the ordered series of measured avalanche durations. Since the PDF of the elements in Q_D^T must be distributed according to an exponential law with the same exponent as the hidden T process, σ_0 can be easily estimated. All the elements in the (somewhat obscure) definition of Q_D^T become now physically meaningful: the t_{s_j} in Eq. (9) correspond to the instants when activity patches start. And the elements in Q_D^T correspond to the lapses of inactivity between these patches, which justifies calling them *quiet times*. (It is interesting to point out that quiet-time statistics can also be useful in other contexts. For instance, the exponential shape of the quiet-time PDF disappears as soon as the recorded triggerings in W^A are no longer decorrelated. This was shown to be possible in Ref. [24], either by using certain types of conditionally sampling the avalanches from a randomly driven system that violates Theorem 2 from Sec. II, or by driving the system with a nonrandom correlated source. The experimental finding of nonexponential quiet-time PDFs in real experiments might thus suggest the relevance of one of these possibilities.)

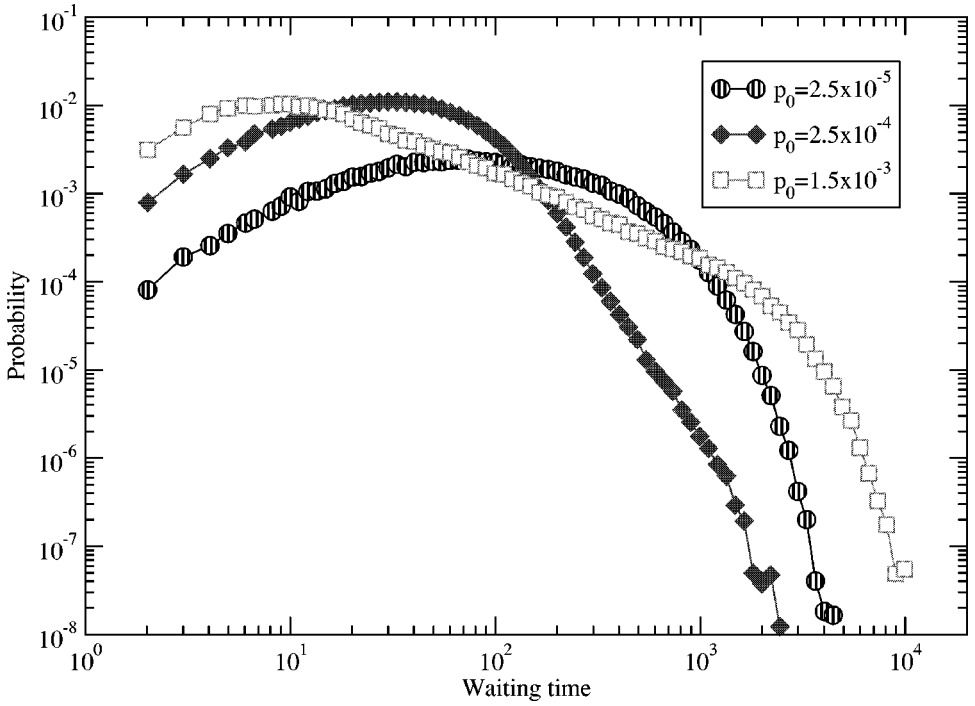

FIG. 4. Change of the PDF according to which the values in W^A are distributed as a function of p_0 for the same case as Fig. 3.

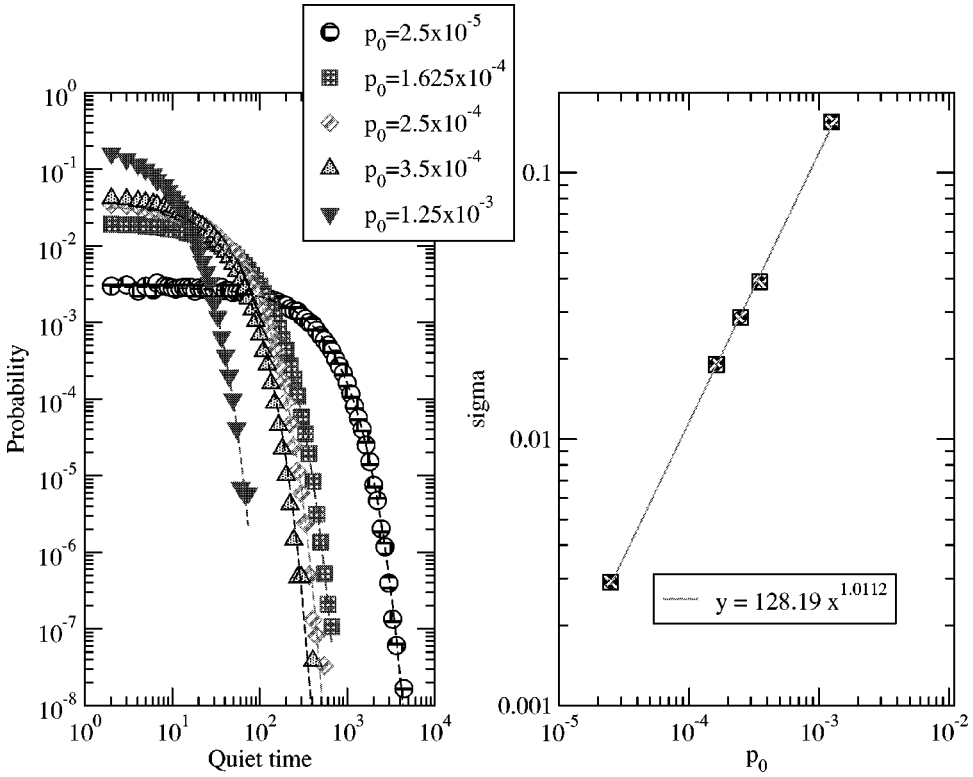

FIG. 5. Statistics of quiet times for a series of sandpile runs with $L=400$ and $N_f=3$ (left). Scaling of σ_0 with p_0 obtained from these cases (right).

IV. ESTIMATION OF p_s FOR THE RUNNING SANDPILE USING QUIET-TIME STATISTICS

In this section, the quiet-time technique described in the two previous sections is used to estimate the dependences and scalings of p_s for the running sandpile. To verify the independence of p_s with respect to p_0, a series of sandpile runs with parameter values given by $L=400$, $Z_c=20$, and $N_f=3$ with increasing p_0 are used (see Fig. 5). In order to test the extent to which quiet-time statistics can yield information about the underlying dynamics when probing within the hydrodynamic regime, the rest of the dependences (i.e., on L and N_f) have been explored using a series of sandpile runs with a value of p_0 well within the strong-overlapping regime. This can be assessed by ascertaining the existence of

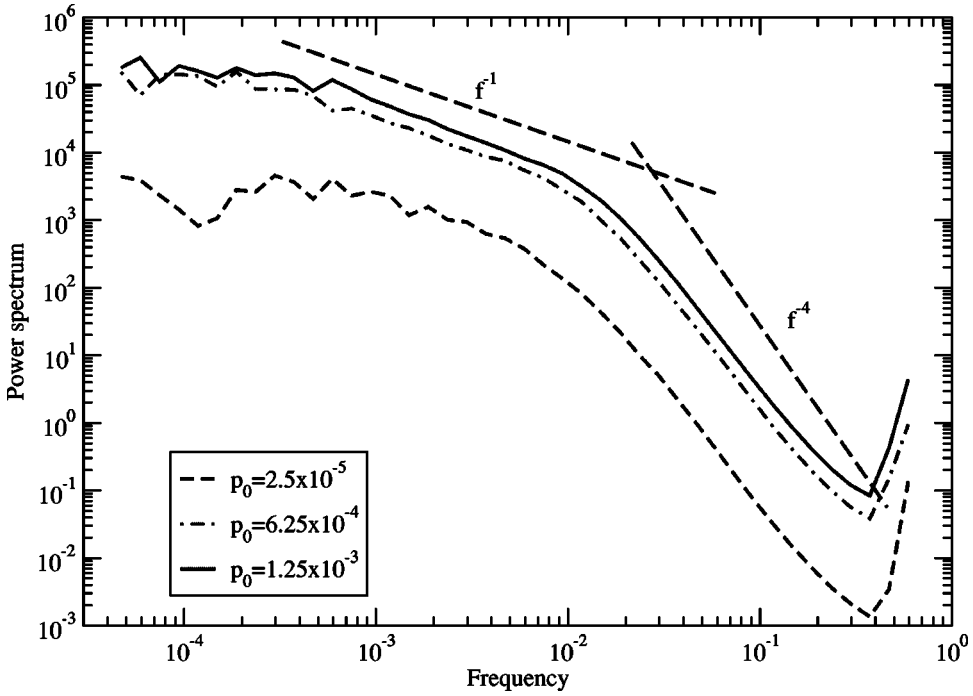

FIG. 6. Power spectra (frequency units are iterations^{-1}) of the time traces of the total number of overturning cells for a series of sandpile runs with $L=400$ and $N_f=3$ and varying drive.

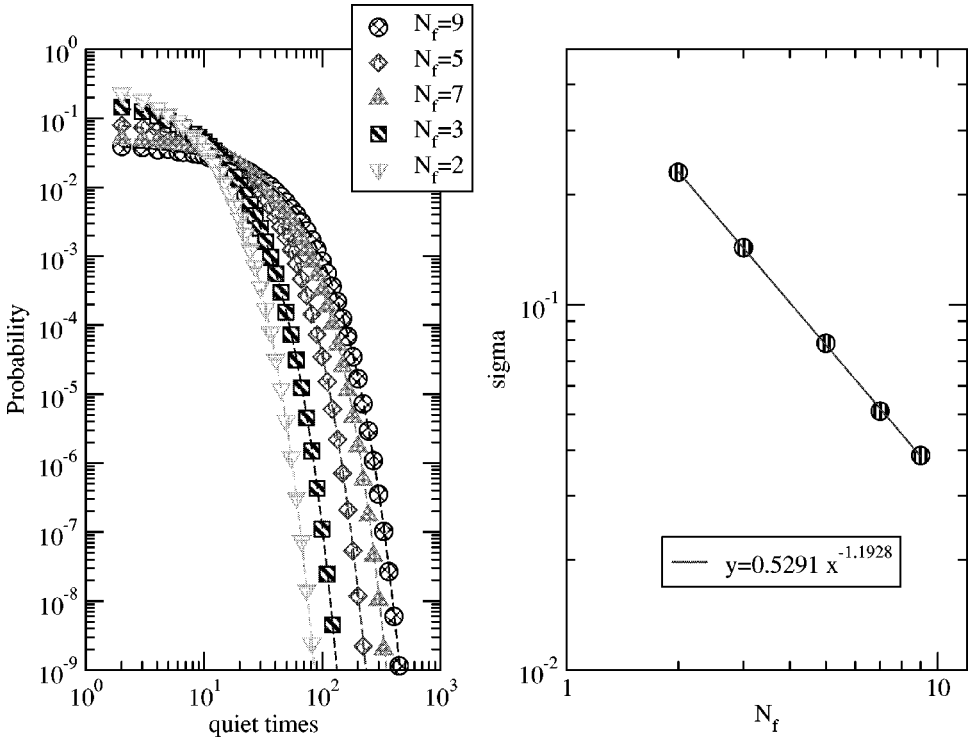

FIG. 7. Statistics of quiet times for a series of sandpile runs with $L=400$ and $p_0=1.25\times10^{-3}$ iteration^{-1} (left). Scaling of σ_0 with N_f obtained from these cases (right).

a wide f^{-1} region in the power spectrum of the time trace for the total number of unstable cells (see Fig. 6), which is well known to be characteristic of the hydrodynamic regime [13]. Assembling data from all these runs, the obtained parametric dependence of p_s turns out to be (see Figs. 7 and 8)

$$\sigma_0=(1.01\pm0.12)\frac{L^{(1.056\pm0.014)}\ p_0^{1.011\pm0.009}}{N_f^{(1.193\pm0.012)}}. \qquad (22)$$

The exponents obtained for both p_0 and L are within the 3–5 % range of deviation expected from the theoretical expectation, $\sigma=p_s p_0 L$. Therefore, the scaling for p_s given by quiet-time statistics in the hydrodynamic regime is

$$p_s \simeq N_f^{-1.2}. \qquad (23)$$

This scaling gives a lower value for p_s than the somewhat naive estimation obtained by assuming that the local slope has an equal probability of staying in any of the stable slope

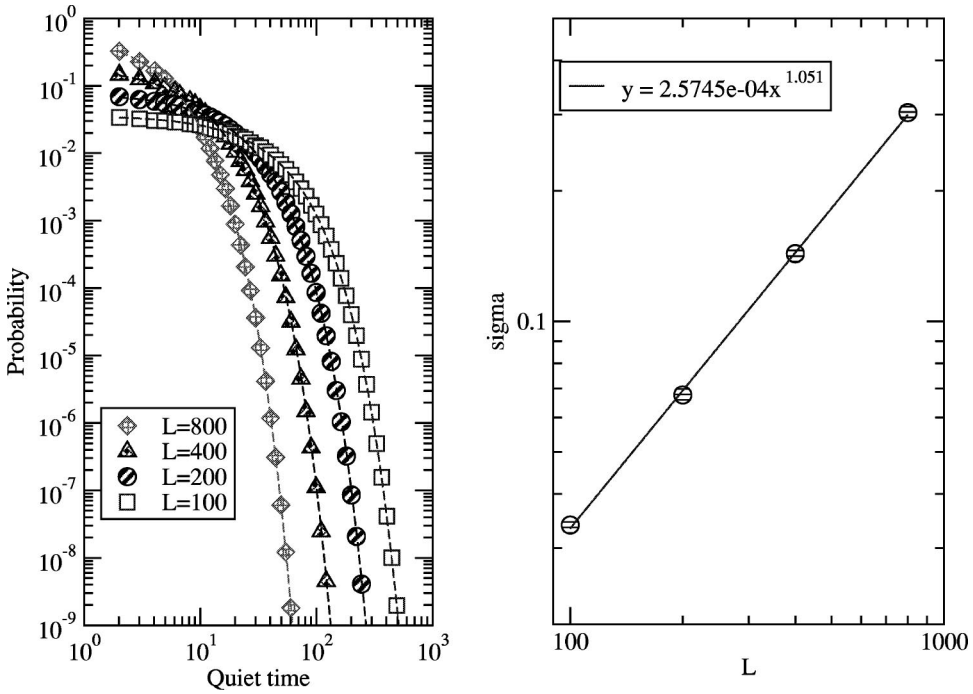

FIG. 8. Statistics of quiet times for a series of sandpile runs with $p_0=1.25\times10^{-3}$ iteration^{-1} and $N_f=3$ (left). Scaling of σ_0 with L obtained from these cases (right).

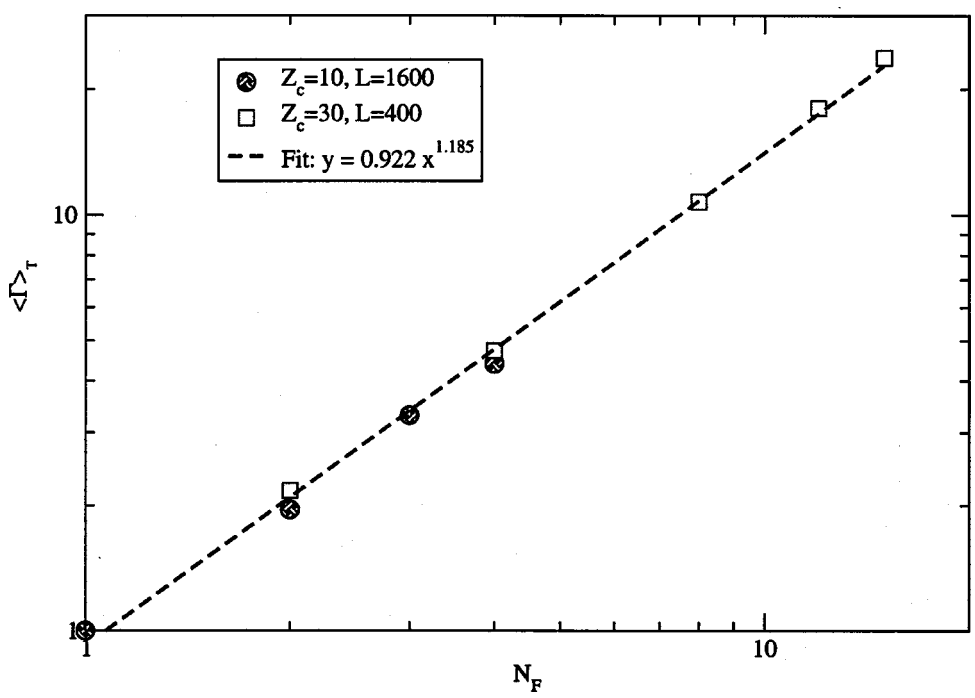

FIG. 9. Scaling of $\langle \Gamma_{out} \rangle_T$ with N_f for the nonoverlapping sandpile.

states within $[Z_c - N_f, Z_c]$, which predicts $p_s = N_f^{-1}$ [24]. The difference in the exponent for N_f is close to 20% with the predicted one, which seems to discard any numerical inaccuracy as responsible for this difference. Thus, Eq. (23) suggests that the previous assumption probably underestimated the importance of the stable slope values lying out of this interval. These values are distributed in $[Z_c - 2N_f, Z_c - N_f]$, and are accessed whenever the first relaxation of an avalanche (that reduces the local slope at the starting location to $Z_c - 2N_f$) does not propagate to other cells (in which case, the local slope is moved up to $Z_c - N_f$ in the following iteration). The influence of these events in the slightly nonlinear scaling (in $1/N_f$) observed seems to be confirmed when neglecting them in the quiet-time statistics, which brings the exponent much closer to linearity (even when their effect on the rest of events is maintained through the modifications of the sandpile profile they cause). The slightly nonlinear dependence could be associated to the radial correlations between the slopes of neighboring cells [27]. They affect these lower-slope states because the slope can be increased towards Z_c not only by a falling grain of sand (that increases the slope in one), but also by means of any avalanche that starts somewhere else and happens to die at this location (increasing the slope by N_f).

V. COMPARISON WITH THE DYNAMICS OF A NONOVERLAPPING SANDPILE

In this section, we are interested in testing the extent to which the information on p_s collected from within the strong-overlapping regime by means of quiet-time statistics reflects any property of the dynamics of the system in the absence of overlapping. Two conservation laws that must hold in the running sandpile will be useful for this task:

$$p_0 L = \sigma_0 \langle \Gamma_{out} \rangle_T, \tag{24}$$

which ensures the flux balance that must hold in steady state, and

$$\frac{p_0 L^2}{2N_f} = \sigma_0 \langle S \rangle_T, \tag{25}$$

which guarantees that all flux in the sandpile is related to avalanche activity. It is important to notice that $\langle \Gamma_{out} \rangle_T$ and $\langle S \rangle_T$, respectively, stand for the average flux out of the pile and the average size (defined as the total number of relaxations that have taken place during the avalanche) per *single* avalanche (even if they may not be distinguished due to overlapping).

Since p_0 cancels out in both sides of Eqs. (24) and (25), these laws hold for any level of overlapping and, in particular, in the limit of no overlapping ($\sigma_0 \to 0$). If the scalings for p_s obtained in the preceding section are correct, it should follow that

$$\langle \Gamma_{out} \rangle_T = \frac{1}{p_s} \simeq N_f^{1.2} \tag{26}$$

and

$$\langle S \rangle_T = \frac{L}{2N_f p_s} \simeq 0.5 \; N_f^{0.2} L. \tag{27}$$

This prediction can be compared with the scalings for both quantities obtained from calculations with a sandpile in which the drive is stopped after an avalanche is excited, being only restarted after all avalanche activity has died away. The obtained scalings are shown in Figs. 9 and 10, agreeing

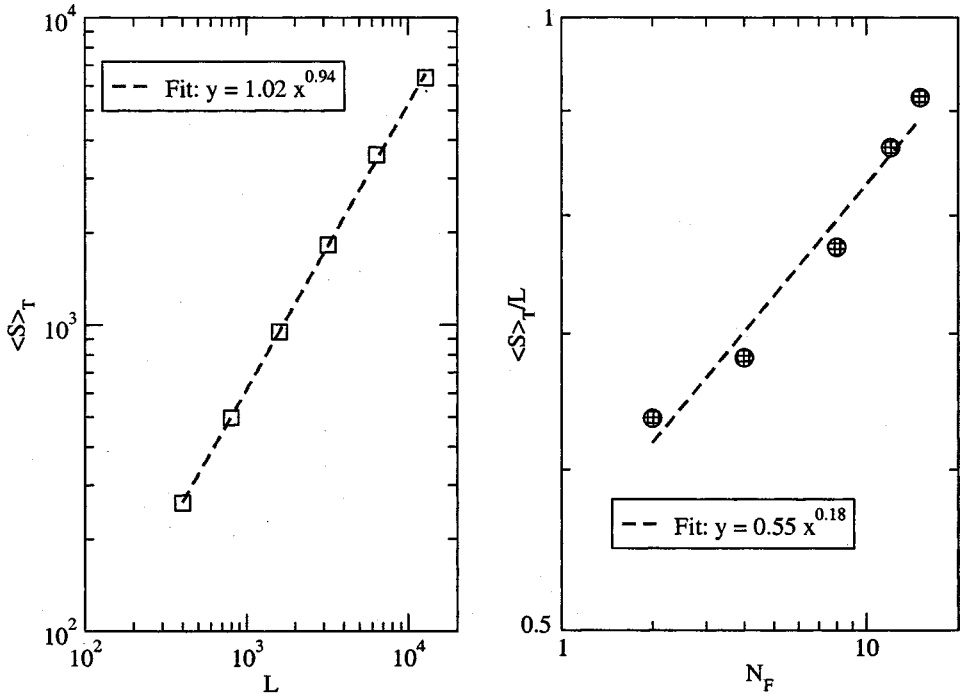

FIG. 10. Scaling of $\langle S\rangle_T$ with L (left, using $N_f=3$ and $Z_c=10$) and of $\langle S\rangle_T/L$ with N_f (right, using $L=400$ and $Z_c=30$) for the nonoverlapping sandpile.

with those provided by quiet-time statistics within less than 5% and confirming the goodness of the method to probe the underlying dynamics.

VI. CONCLUSIONS

In this paper we have shown that quiet-time statistics can be a powerful tool to test the underlying dynamics of randomly driven SOC systems, even if measurements can only be made in the hydrodynamic regime where avalanches cannot be clearly separated. This result extends importantly to the regimes in which these systems can be probed, since it is no longer required to go to the limit of vanishing drive (i.e., $p_0 \to 0^+$) to obtain precise information about their dynamics. In particular, it can be of significant importance in real physical systems in which, in contrast to the running sandpile used to test the method, the level of overlapping cannot be easily controlled and where the diagnostics available are also very limited. This is certainly the case in magnetically confined plasmas. In them, the combination of short discharges and extremal conditions allows, at most, for measurements providing the flux coming out of the system or through some fixed radial location. In systems like these, the results described in the paper may be of application to obtain information about the underlying dynamics.

ACKNOWLEDGMENTS

Valuable discussions with M. Varela, U. Bhatt, and R. Woodard are acknowledged. The research was supported in part by the Spanish DGES Project No. FTN2000-0965 and by the Office of Fusion Energy, U.S. DOE, under Contracts No. DE-AC05-00OR22725 and No. DE-FG03-99ER54551.

[1] P. Bak, C. Tang, and K. Wiesenfeld, Phys. Rev. Lett. **59**, 381 (1987).
[2] J.M. Carlson and J.S. Langer, Phys. Rev. Lett. **62**, 2632 (1989).
[3] E. Lu and R.J. Hamilton, Astrophys. J. **380**, L89 (1991).
[4] B. Drossel and F. Schwabl, Phys. Rev. Lett. **69**, 1629 (1992).
[5] P. Bak and K. Sneppen, Phys. Rev. Lett. **71**, 4083 (1993).
[6] S. Mineshige, M. Takeuchi, and H. Nishimori, Astrophys. J. **435**, L125 (1994).
[7] S. Field, J. Witt, and F. Nori, Phys. Rev. Lett. **74**, 1206 (1995).
[8] T. Nagatani, Physica A **218**, 145 (1995).
[9] P.H. Diamond and T.S. Hahm, Phys. Plasmas **2**, 3640 (1995).
[10] D.E. Newman, B.A. Carreras, and P.H. Diamond, Phys. Lett. A **218**, 58 (1996).
[11] L.P. Kadanoff, S.R. Nagel, L. Wu, and S.M. Zhou, Phys. Rev. A **39**, 6524 (1992).
[12] S.S. Manna, L.B. Kiss, and J. Kertesz, J. Stat. Phys. **61**, 923 (1990).
[13] T. Hwa and M. Kardar, Phys. Rev. A **45**, 7002 (1992).
[14] K. Christensen and Z. Olami, J. Geophys. Res. **97**, 8729 (1992).
[15] A.A. Middleton and C. Tang, Phys. Rev. Lett. **74**, 742 (1995).
[16] R. Dickman, A. Vespignani, and S. Zapperi, Phys. Rev. E **57**, 5095 (1998).
[17] B.A. Carreras, V.E. Lynch, D.E. Newman, and G.M. Zaslavsky, Phys. Rev. E **60**, 4770 (1999).
[18] R. Sánchez, D.E. Newman, and B.A. Carreras, Nucl. Fusion **41**, 247 (2001).
[19] H.J. Jensen, *Self-Organized Criticality* (Cambridge University Press, Cambridge, 1998).

[20] B.A. Carreras, D.E. Newman, V.E. Lynch, and P.H. Diamond, Phys. Plasmas **3**, 2903 (1996).
[21] P.A. Politzer, M.E. Austin, M. Gilmore, G.R. McKee, T.L. Rhodes, C.X. Yu, E.J. Doyle, T.E. Evans, and R.A. Moyer, Phys. Plasmas **9**, 1962 (2002).
[22] M.S. Wheatland, P.A. Sturrock, and J.M. McTiernan, Astrophys. J. **509**, 448 (1998).
[23] G. Boffetta, V. Carbone, P. Giuliani, P. Veltri, and A. Vulpiani, Phys. Rev. Lett. **83**, 4662 (1999).
[24] R. Sánchez, D.E. Newman, and B.A. Carreras, Phys. Rev. Lett. **88**, 068302 (2002).
[25] D.R. Cox and V. Isham, *Point Processes* (Chapman and Hall, London, 1980).
[26] J.F.C. Kingman, *Poisson Processes* (Oxford University Press, Oxford, 1993).
[27] B.A. Carreras, V.E. Lynch, D.E. Newman, and R. Sánchez, Phys. Rev. E **66**, 011302 (2002).